Progress of Theoretical Physics Supplement No. 159, 2005

Dilute *Kagomé* Lattice Magnetism with $S = 1/2$ on $Rb_2(Pd_{1-x}M_x)_3S_4$(M = Co, Mn)

Ryota KUKI,[1] Yoshihiro FUJIWARA,[1] Toshio ONO,[1] Katsunori IIO,[1]
Makoto TACHIBANA,[2] Toru ATAKE[2] and Yumi NAKAI[3]

[1]*Department of Physics, Graduate School of Science and Engineering,*
Tokyo Institute of Technology, Tokyo 152-8551, Japan
[2]*Materials and Structures Laboratory Tokyo Institute of Technology,*
Yokohama 226-8503, Japan
[3]*Application and Research Center JEOL.LTD., Akisima 196-8558, Japan*

An attempt to substitute Co^{2+}, Mn^{2+} for Pd^{2+} was performed to yield dilute *kagomé* lattice magnetism of $S = 1/2$ on a ternary transition metal chalocogenide $Rb_2Pd_3S_4$. This compound takes a crystal structure, Pd sites of which constitute *kagomé* lattice nets. Because the divalent $Pd^{2+}(4d)^8$'s on the *kagomé* lattice are in a low-spin state of spin-less owing to specific characteristics of the crystal field influencing on the Pd sites. Magnetic properties of specimens thus obtained were examined through magnetic susceptibility, ESR and specific heat measurements. Several data were obtained for confirming the syntheses of $S = 1/2$ systems in spite of dilute magnetic ones with substitutional ratio x's below the site percolation threshold $x_p = 0.62$ of the *kagomé* lattice.

§1. Introduction

Inspecting the crystal structure analyses in ternary metal chalocogenide $A_2B_3S_4$ (A = K, Cs, Rb, B = Ni, Pd, Pt) carried out by Bronger et al.,[1),2)] our group once noticed that Ni or Pd in $Rb_2Ni_3S_4$ and $Rb_2Pd_3S_4$ constitute typical *kagomé* lattice nets. As shown in Figs. 1 and 2, the one Pd^{2+} site is distinguished crystallographically from the other. However the two sites are geometrically identical on a Pd^{2+} layer and thus the crystal structure is characterized by Pd^{2+} layers of

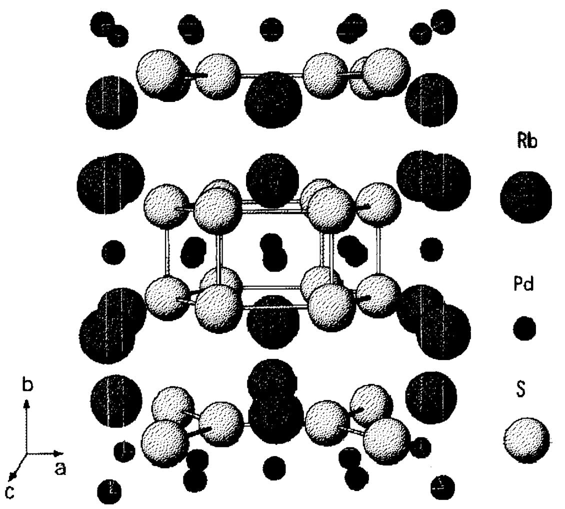

Fig. 1. The unit cell of $Rb_2Pd_3S_4(Fmmm)$.

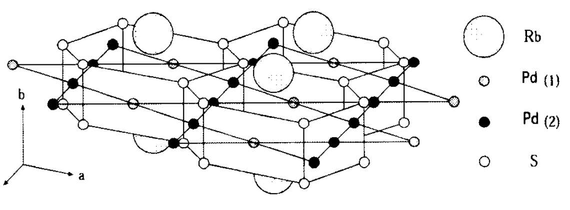

Fig. 2. A stacked package of $Rb_2Pd_3S_4$.

a *kagomé* lattice along the *b* axis. If the Pd^{2+} sites are magnetic and the interactions between them are antiferromagnetic, strong spin frustration originated from a geometrical restriction may be demonstrated. We measured magnetic and electric transport properties of their single crystals grown by a flux method and observed weak ferromagnetic behavior at low temperatures in the Ni^{2+} system with $(3d)^8$.[3] Then we had interest in the $A_2B_3S_4$ systems from a viewpoint of *kagomé* lattice magnetism and subsequently knew a report by Elder et al. that $K_2Ni_3S_4$ (a stacking sequence of the stacked package along the *b* axis is slightly different from that in $Rb_2Ni_3S_4$) exhibits the magnetic behavior similar as $Rb_2Ni_3S_4$ and this origin may be attributable to valence fluctuation in Ni ions.[4] However, after elaborating sample preparation with special care, we revealed that the intrinsic crystal is a band-like insulator with spin less, namely, the electronic configuration of $(3d)^8$ on Ni^{2+} takes a low spin state as a reflection of the crystalline field from the planar $(S^{2-})_4$ ligands under the strong covalency between Ni^{2+} and S^{2-}, where the electronic state specified by one of the d_γ-orbital has a level far above other four $3d$-orbitals.[5] It was also reported from a MNR study that the observed weak magnetism is extrinsic.[6] In this way a possibility to find novel magenetic features in those systems seemed to be lost.

However, a theoretical calculation of local density approximation for the electronic structure of $Rb_2Ni_3S_4$ performed by Usuda et al. showed that an electronic state just below the Fermi level E_F may constitute a flat band specific to *kagomé* lattice and appropriate carrier-doping on the host lattice can derive novel magnetic and transport properties.[7],[8] Through those studies, the Pd^{2+} system with $(4d)^8$ was empirically shown to remain non-magnetic regardless of sample preparation process. Therefore, we attempted to substitute $Co^{2+}(3d)^7$, $Mn^{2+}(3d)^5$ for $Pd^{2+}(4d)^8$ for yielding some novel magnetism on the host *kagomé* lattice despite of dilute magnetic systems. In this approach, the reason why $3d$-transition metals were chosen instead of $4d$-transition metal element of Rh or Tc is that the ionic radii of the former $3d$ transition metals are smaller than those of the latter $4d$ ones and the substitution can be easily carried out.[9] If Co^{2+} or Mn^{2+} are successfully introduced in the host lattice, their spin moments are expected to behave as $S = 1/2$ quantum spins.

§2. Experimental procedures

Powder specimens of $Rb_2\,(Pd_{1-x}M_x)_3S_4$ (M = Co, Mn) were grown by a flux method, for the detailed of which one refers to Ref. 5). Crystal quality of specimens thus prepared was proved to be satisfactory by examining powder X-ray diffraction patterns of both the host and the substituted systems, where an X-ray source of Cu Kα was employed. ESR spectra were obtained at room temperature and liquid-nitrogen temperature with an ESR spectrometer of the X-band (JEOL, JES-FA200) by recording the differential absorption intensity as a function of magnetic field. The temperature dependence of magnetic susceptibility was measured down to 1.8 K under applied fields up to 7 T with a SQUID magnetometer (Quantum Design MPMS XL). The specific heat measurements were performed by the use of a physical-property measurement system (Quantum Design, PPMS) in a temperature range from 2 K to 300 K.

§3. Experimental results

Figures 3 and 4 show ESR differential line-profiles in powder crystals for two kinds of dilute systems, respectively. For a typical Co^{2+}-doped system, the main resonance absorption was observed at a field indicating the $g_\perp$ factor of 2.05, which supports the doped Co^{2+} taking the low-spin state. Furthermore, as seen in the figure, another subsidiary absorption was observed at the position where the $g_\parallel$ factor is 2.66. This line profile for the powder specimen implies that the magnetic moments of doped Co^{2+} have uniaxial anisotropy. For a typical Mn^{2+}-doped system, we observed the main absorption of the g factor of 2.006 together with a hyperfine resonance absorption ascribed probably to the excitation of the spin-triplet state of a coupled $S = 1/2$ spin pair appearing at the field nearly half with respect to the main resonance. Since the resonance absorption spectrum obtained by integrating numerically the differential one is ascertained to be represented well with a Lorenzian profile, the exchange narrowing of the linewidth for the main resonance is promoted by the exchange interactions between Mn pairs, where their presence is supported with the observation of the triplet excitation.

The magnetic susceptibility χ measured under an applied field of 0.1 T as a function of temperature together with its inverse $1/\chi$ and the magnetization M at $T = 2$ K as a function of magnetic filed are shown in Figs. 5 and 6. The $1/\chi(T)$ vs T plots indicate that the dominant nearest-neighbor interaction between the Co^{2+} spins and that between the Mn^{2+} ones are both antiferromagnetic. Ferromagnetic-like spin ordering is seen in the Co^{2+}-doped system, though no sign of such ordering was observed for the Mn^{2+}-doped one. Since those plots exhibited linear behavior about above 150 K, the Weiss temperature $\Theta_{\rm Weiss}$'s were determined from the extrapolation of the slope to $1/\chi(T) = 0$ to be -40 K and -690 K for the Co^{2+} and Mn^{2+} specimens, respectively. In addition, the spin value estimated from the Curie constant by using the equation: $S(S+1) = 3k_{\rm B}C_{\rm Curie}/Ng^2\mu_{\rm B}^2$ were 0.34, 0.55 for the Co^{2+}, Mn^{2+} specimenss, respectively, so as to support that those doped spins are in the low-spin state with S of 1/2, though the magnitude of the former was rather smaller than 0.5.

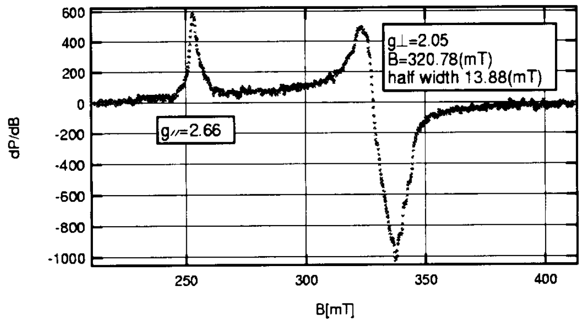

Fig. 3. ESR spectra of $Rb_2(Pd_{0.42}Co_{0.58})_3S_4$ obtained at room temperature.

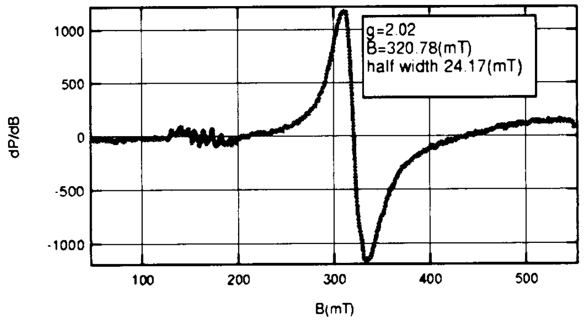

Fig. 4. ESR spectra of $Rb_2(Pd_{0.95}Mn_{0.05})_3S_4$ obtained at liq. N_2 temperature.

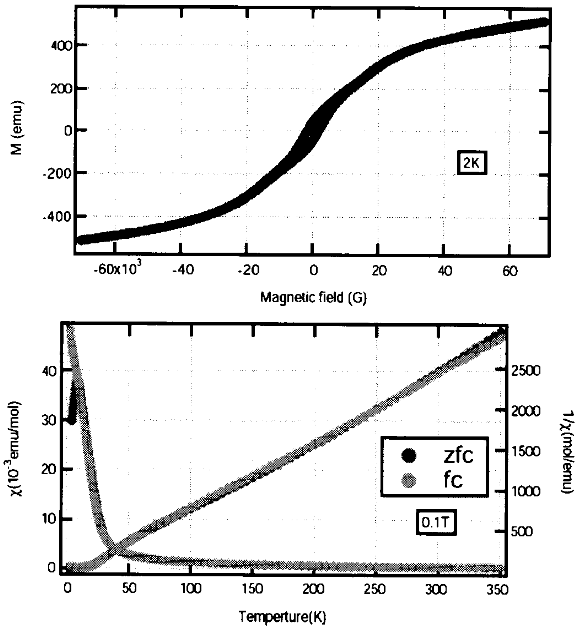

Fig. 5. M vs H, χ vs T and $1/\chi$ vs T curves of $Rb_2(Pd_{0.79}Co_{0.21})_3S_4$.

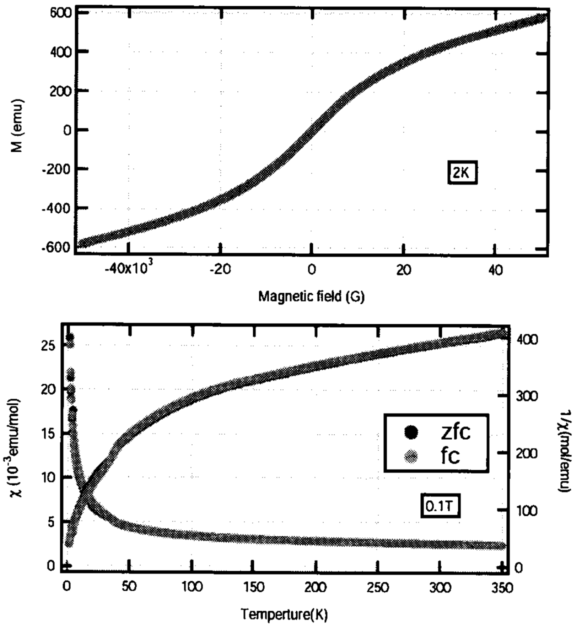

Fig. 6. M vs H, χ vs T and $1/\chi$ vs T curves of $Rb_2(Pd_{0.70}Mn_{0.30})_3S_4$.

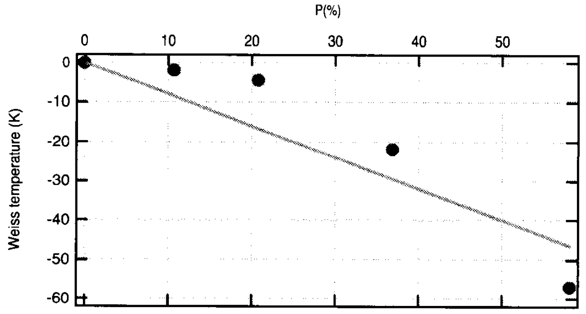

Fig. 7. $\Theta_{\mathrm{Weiss}}(x)$ vs x for $Rb_2\ (Pd_{1-x}Co_x)_3S_4$.

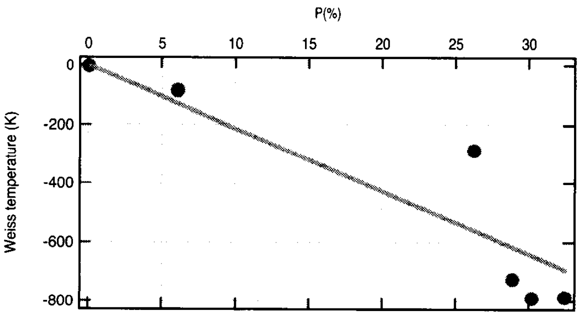

Fig. 8. $\Theta_{\mathrm{Weiss}}(x)$ vs x for $Rb_2\ (Pd_{1-x}Mn_x)_3S_4$.

From the $1/\chi(T)$ vs T plots above 150 K for mixtures with several Co^{2+} or Mn^{2+} concentrations, x of which is up to about 0.5 for the Co^{2+} systems and up to about 0.3 for the Mn^{2+} ones, the Weiss temperatures of the specimens as a function of x, $\Theta_{\mathrm{Weiss}}(x)$, were deduced. Then, based on the plots of $\Theta_{\mathrm{Weiss}}(x)$ vs x shown in Figs. 7 and 8, the dominant exchange constant J/k_{B}'s were evaluated, in terms of the equation: $J/k_{\mathrm{B}} = 3\Theta_{\mathrm{Weiss}}/2Z(x)S(S+1)$, to be ~ -40 K(Co^{2+}), ~ -1040 K(Mn^{2+}), respectively. In this approach, the number Z of the nearest site was supposed to be linearly dependent of x. Since an adequate straight line through the data points can be drawn in each $\Theta_{\mathrm{Weiss}}(x)$ vs x, this approximation is substantiated within the doped range of x.

From a specific heat measurement for a Mn^{2+} sample illustrated in Figs. 9 and 10, the temperature dependence of $C(T)$ was found to obey $C(T) = \gamma T + AT^3$. Although the presence of an unusual T^2 dependence in $C(T)$ was reported for some $S = 1/2$ quantum *kagomé* spin systems,$^{10)}$ no such a term of T^2 was identified with in the present measurement. We have at present a plan to carry out further measurements at lower temperatures on specimens with other substitutional ratios.

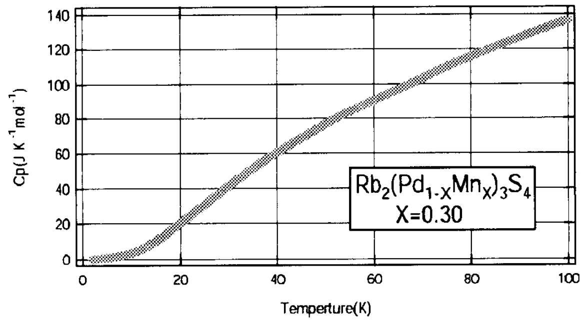

Fig. 9. Specific heat of $Rb_2(Pd_{0.70}Mn_{0.30})_3S_4$ down to 2 K.

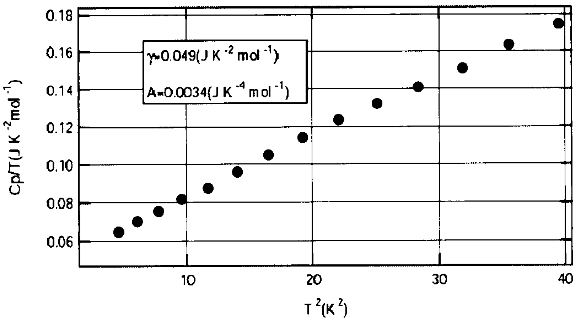

Fig. 10. C/T vs T^2 plots of $Rb_2(Pd_{0.70}Mn_{0.30})_3S_4$.

§4. Discussion and conclusions

Although the specimens obtained had x's below the site percolation threshold $x_p = 0.62$ of a *kagomé* lattice, partial doping of Co^{2+} or Mn^{2+} was successfully made in the host $Rb_2Pd_3S_4$. The magnetic susceptibility and ESR measurements confirm that the doped Co^{2+} and Mn^{2+} take an low-spin state so as to behave as the quantum spin of 1/2. The susceptibility measurements show that the interaction between Co^{2+}'s and also Mn^{2+}'s are antiferromagnetic. Some ordering behavior observed in the Co^{2+}-doped specimens could not be ascertained in the Mn^{2+}-doped one, though the dominant interaction of the latter is fairly larger than that of the former. We presume those facts to be certainly a unique feature of highly frustrated systems. The reasons why such a fairly strong antiferromagnetic interaction is active between the Mn^{2+} pairs and also why the spin ordering occurs in the Co^{2+} system at temperatures below about 20 K have to be clarified. The ESR signal indicating uniaxial anisotropy was observed for the Co^{2+} system, whereas no such spectrum was observed for the Mn^{2+} one. It is necessary to examine whether the uniaxial character in the Co^{2+} system is responsible for the magnetic anomaly at low temperatures. Because Kuroda and Miyashita predicted theoretically for a *kagomé* lattice antiferromagnet that the systems of Heisenberg spin with a weak Ising-like anisotropy exhibit nontrivial ferromagnetic order perpendicular to a *kagomé* plane.[11] This scenario may be applicable to the present Co^{2+} doped system.

However, for reasonable discussion on those problems, systems with x of Mn^{2+} near the percolation threshold should be synthesized, to begin with, to ascertain presence or absence of such magnetic anomaly. It should be also acknowledged through growing of large single crystals that the easy-axis anisotropy is surely perpendicular to the Co^{2+} *kagomé* plane. Furthermore, based on a naive crystal field picture without the covalent effect of Pd located at the center of the S_4 square, the doped Co^{2+} with $(3d)^7$ in a low spin state has no orbital degeneracy and the orbital degeneracy remains in such Mn^{2+} with $(3d)^5$. It follows that the Mn system can have magnetic anisotropy instead of the Co one. If the electronic state of Co^{2+} and Mn^{2+} are analyzed by taking properly the covalency within the MS_4 (M = Co, Mn) clusters into account, this discrepancy between the empirical results and the supposition may be resolved. Then fairly large superexchange coupling between a Mn pair on this lattice will be justified theoretically. Further experimental and theoretical approaches are required to clarify the present subject.

Acknowledgements

We are indebted to Dr. Katsuhiro Hondou for meaningful advice on the present study.

References

1) J. Huster and W. Bronger, J. Solid State Chem. **11** (1974), 254.
2) W. Bronger and P. Muller, J. Less-Common Metals **100** (1984), 241.
3) T. Kato, K. Hondou and K. Iio, J. Magn. Magn. Mater. **177** (1998), 591.
4) S. H. Elcder, S. Jobic, R. Brec, M. Gelabert and F. J. Disalvo, J. Alloys Comp. **235** (1998), 135.
5) K. Hondou, Y. Fujiwara, T. Kato, K. Iio, A. Saiki, M. Usuda and N. Hamada, J. Alloys Comp. **333** (2002), 274.
6) T. Fukamachi, Y. Kobayashi, A. Nakamura, H. Harashina and M. Sato, J. Phys. Soc. Jpn. **68** (1999), 3668.
7) M. Usuda and N. Hamada, Read at annual meeting of Phys. Soc. Jpn., Tokushima (2001) 17pPSB-25.
8) K. Hondou, M. Usuda and K. Iio, Ceramics-Silikáty **49** (2005), 1.
9) Y. Fujiwara, Master's thesis, Tokyo Institute of Technology (2002).
10) A. P. Ramirez, G. P. Espinosa and A. S. Cooper, Phys. Rev. B. **45** (1992), 2505.
11) A. Kuroda and S. Miyashita, J. Phys. Soc. Jpn. **64** (1995), 4509.